Interference effects of choice on confidence: Quantum characteristics of evidence accumulation

Peter D. Kvam[a,b,1], Timothy J. Pleskac[b,1], Shuli Yu[a], and Jerome R. Busemeyer[c]

[a]Department of Psychology, Michigan State University, East Lansing, MI 48824; [b]Center for Adaptive Rationality, Max Planck Institute for Human Development, 14195 Berlin, Germany; and [c]Department of Psychological and Brain Sciences, Indiana University, Bloomington, IN 47405

Edited by James L. McClelland, Stanford University, Stanford, CA, and approved July 10, 2015 (received for review January 13, 2015)

Decision-making relies on a process of evidence accumulation which generates support for possible hypotheses. Models of this process derived from classical stochastic theories assume that information accumulates by moving across definite levels of evidence, carving out a single trajectory across these levels over time. In contrast, quantum decision models assume that evidence develops over time in a superposition state analogous to a wavelike pattern and that judgments and decisions are constructed by a measurement process by which a definite state of evidence is created from this indefinite state. This constructive process implies that interference effects should arise when multiple responses (measurements) are elicited over time. We report such an interference effect during a motion direction discrimination task. Decisions during the task interfered with subsequent confidence judgments, resulting in less extreme and more accurate judgments than when no decision was elicited. These results provide qualitative and quantitative support for a quantum random walk model of evidence accumulation over the popular Markov random walk model. We discuss the cognitive and neural implications of modeling evidence accumulation as a quantum dynamic system.

confidence | Markov | decision-making | cognitive model | random walk

Decisions in a wide range of tasks (e.g., inferring the presence or absence of a disease, the guilt or innocence of a suspect, and the left or right direction of enemy movement) require evidence to be accumulated in support of different hypotheses. Arguably, the most successful theory of evidence accumulation in humans and other animals is Markov random walk (MRW) theory (and diffusion models, their continuous space extensions) (1, 2). MRWs can be viewed as psychological implementations of a first-order Bayesian inference process that assigns a posterior probability to each hypothesis (3). MRWs can account for choices, response times, and confidence for a variety of different decision types (2, 4). Moreover, these models of the accumulation process have been connected to neural activity during decision-making (5, 6).

According to MRW models, when deciding between two hypotheses, the cumulative evidence for or against each hypothesis realizes different levels at different times to generate a single particle-like trajectory of evidence levels across time (Fig. 1). At any point in time, the decision-maker has a definite level of evidence, and choices are made by comparing the existing level of evidence against a criterion. Evidence above the criterion favors one option, and evidence below it favors the alternative. Other responses are modeled in a similar manner; for example, confidence ratings are modeled by mapping evidence states onto one or more ratings (4). However, this idea that judgments and decisions are simply read out from the existing level of evidence—henceforth referred to as the "read-out" assumption—is inconsistent with the well-established idea that preferences and beliefs are constructed rather than revealed by judgments and decisions (7).

We present an alternative model of choice and judgment based on quantum random walk (QRW) theory (8–11), which posits that preferences and beliefs are constructed when a judgment or decision is made. Note that this work does not make the assumption that the brain is a quantum computer; instead, we simply use the mathematics of quantum theory to explain and predict human behavior. According to QRW theory, at any point in time before a decision, the decision-maker is in a superposition state that is not located at a single level of evidence. Instead, each level of evidence has a potential to be expressed, formalized as a probability amplitude (Fig. 1). New information changes the amplitudes, producing a wavelike process that moves the amplitude distribution across time.

In some ways the QRW is like a second-order Bayesian model (12). According to the latter, the decision-maker assigns a probability (rather than an amplitude) to each level of evidence for each hypothesis. However, like the MRW model, second-order Bayesian models are perfectly compatible with the read-out assumption, and as an optimal model, this would suggest that a decision should not change the probability assigned to each evidence level. In contrast, a QRW, like all quantum models of cognition (13), treats a judgment or decision as a measurement process that constructs a definite state from an indefinite (superposition) state. When a decision is made, the indefinite state collapses onto a set of evidence levels that correspond to the observed choice, producing a definite choice state. Confidence ratings work similarly, with the indefinite state collapsing onto a more specific set of levels corresponding to the observed rating.

These different theories of choice and judgment have strong implications for sequences of responses. Consider the situation when decision-makers have to make a choice (e.g., decide that hypothesis A or B is true) and later rate their confidence that a given (usually the chosen) hypothesis is true. According to the read-out assumption, a choice is reported on the basis of existing evidence that does not change the internal state of evidence itself. This applies to the MRW, a second-order Bayesian model, and many other accumulation models as well. Thus, after pooling across a person's choices, the distribution of confidence ratings should be identical to conditions in which the person makes no choice at all. By contrast, the state of the system in a QRW

Significance

Most cognitive and neural decision-making models—owing to their roots in classical probability theory—assume that decisions are read out of a definite state of accumulated evidence. This assumption contradicts the view held by many behavioral scientists that decisions construct rather than reveal beliefs and preferences. We present a quantum random walk model of decision-making that treats judgments and decisions as a constructive measurement process, and we report the results of an experiment showing that making a decision changes subsequent distributions of confidence relative to when no decision is made. This finding provides strong empirical support for a parameter-free prediction of the quantum model.

Author contributions: P.D.K., T.J.P., and J.R.B. conceived of the study; P.D.K., T.J.P., .S.Y., and J.R.B. designed the research; P.D.K. ran the study; P.D.K. and T.J.P. analyzed data; P.D.K., T.J.P., S.Y., and J.R.B. wrote the paper; and T.J.P. supervised all aspects of the work.

The authors declare no conflict of interest.

This article is a PNAS Direct Submission.

Freely available online through the PNAS open access option.

[1]To whom correspondence may be addressed. Email: kvam.peter@gmail.com or pleskac@mpib-berlin.mpg.de.

This article contains supporting information online at www.pnas.org/lookup/suppl/doi:10.1073/pnas.1500688112/-/DCSupplemental.

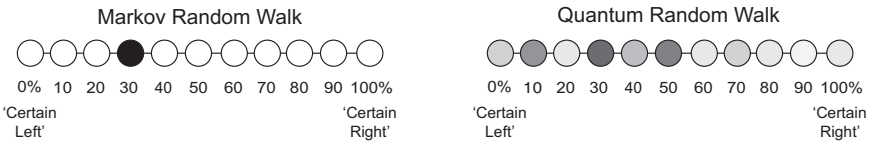

Fig. 1. Diagram of a state representation of a Markov and a quantum random walk model. In the Markov model, evidence (shaded state) evolves over time by moving from state to state, occupying one definite evidence level at any given time. In the quantum model the decision-maker is in an indefinite evidence state, with each evidence level having a probability amplitude (shadings) at each point in time.

is changed when a choice creates a definite state. Subsequent processing starts from the definite state, and the amplitudes spread out again. Thus, if information processing continues after the initial stage, the QRW predicts an interference effect where the marginal distribution of confidence judgments following a choice will differ from a condition in which no choice is made.

A proof of the predicted interference effect for QRWs is in *SI Appendix*. The proof shows that the interference effect of choice on confidence is the result of the interaction between the creation of a definite state and subsequent evidence accumulation after making a choice. Subsequent or second-stage processing is a necessary condition for the effect. Critically, second-stage processing occurs when people are asked to report a confidence rating following a choice, giving rise to response reversals (14) and other properties (15). We also provide a proof that MRWs predict no difference between the marginal distributions of confidence ratings (i.e., no interference) regardless of the presence of second-stage processing. This proof holds for a large range of MRWs, including ones with decay (16), leakage of evidence (17), and trial-by-trial variability in the decision process (18).

Empirical Test of Predicted Interference Effect

We tested these opposing predictions concerning interference effects using a perceptual task that requires participants to judge the direction of motion in a dynamic dot display (Fig. 2). Specifically, nine participants completed 112 blocks of 24 trials each over five 1-h experimental sessions, a total of 2,688 trials per person (*SI Appendix*). During each trial, participants viewed a random dot motion stimulus that consisted of moving white dots in a circular aperture on a black background (19). A percentage of the dots moved coherently in one direction (left or right), and the rest moved randomly. Difficulty was manipulated between trials by changing the percentage of coherently moving dots (2%, 4%, 8%, or 16%). In the choice condition—half of the randomly ordered blocks—participants were prompted 0.5 s from stimulus onset via a low-frequency beep (400 Hz) to decide whether the coherently moving dots were moving left or right and entered their choice by clicking the corresponding mouse button. In the no-choice condition—the other half of the blocks—participants were prompted 0.5 s from stimulus onset via a high-frequency beep (800 Hz) to make a motor response (click the left or right mouse button as instructed). In all trials, the stimulus remained on screen for a second stage of processing after the choice or click. After an additional 0.05, 0.75, or 1.5 s following the first response, participants were prompted via a second beep (400 Hz) to rate their confidence that the coherently moving dots were moving right on a semicircular scale that appeared at the time of the prompt, ranging from 0 (certain left) to 100% (certain right) in unit steps. Note that to match the overall processing time of the stimulus across conditions, the confidence prompt was time-locked to the initial choice or click entry.

For the behavioral analyses, we collapsed confidence responses across the dot motion direction, recoding confidence onto a half scale (50% guess to 100% certain). All behavioral analyses were conducted using hierarchical Bayesian general linear models (20). The coefficient b is the linear effect of a predictor on the criterion. We also report the highest density interval (HDI) for all estimates, which specifies the range covering the 95% most credible values of the posterior estimates. A normal link was used for confidence judgments after transforming them to log odds, and a logistic link was used for choices.

On average, confidence increased with motion coherence ($b = 0.66$; 95% HDI = [0.31, 1.02]). In the choice condition, the proportion of correct choices increased with coherence ($b = 0.50$; 95% HDI = [0.04, 1.16]). Confidence judgments were, on average, lower in the choice ($M = 83.96$; $SD = 15.56$) than in

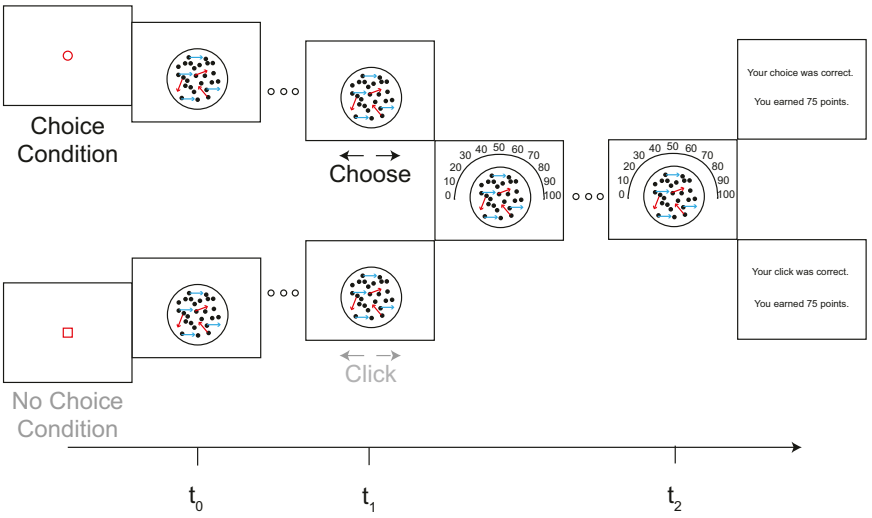

Fig. 2. Diagram of the task. A fixation point indicated the choice/no-choice condition, then the stimulus was shown for 0.5 s. A prompt (t_1) then asked for a decision on the direction of the dot motion (choice condition) or a motor response (no-choice condition). The stimulus remained on the screen. A second prompt (t_2) then asked for a confidence rating on the direction of the dot motion. Finally, feedback was given on the accuracy of their responses.

the no-choice condition ($M = 85.15; SD = 14.95$); the value of the interference main effect coefficient is reported at the individual and group level in Table 1 (see also *SI Appendix*, Table S1). *SI Appendix*, Figs. S1 and S6 also show this effect at the distribution level. This effect of choice on confidence provides evidence against the read-out assumption and is consistent with the quantum claim that choice changes the state of the cognitive system.

We also examined the QRW prediction that the interference effect does not occur with choice alone but that the interaction between choice and subsequent processing creates interference. To gauge whether participants were sampling information during the second stage, we examined whether there was an interaction between coherence and duration of the second stage when confidence was predicted on a full scale from 0 (completely sure, incorrect direction) to 100 (completely sure, correct direction). The magnitude of this coefficient indicates second-stage processing under the following logic: on average, people sample information in favor of the correct answer during this second stage, and this evidence should be stronger with higher coherence (drift), resulting in an interaction between coherence and the duration of the second stage.

The value of this second-stage processing interaction coefficient is reported in Table 1. With the exception of participant 3, there is a 1:1 correspondence between credible second-stage processing and a credible interference effect. Note that participant 3 is by several measures an anomaly: this participant was unable to distinguish between dot motion directions in most conditions and in fact had lower than 50% correct choices in some conditions (*SI Appendix*, Fig. S4).

Further evidence for the requirement of second-stage processing comes from a study in which we failed to obtain interference when no second-stage processing was induced. This study was almost identical to the one described above, with two differences: first, there was no trial-by-trial feedback, and second, the decision time was 0.8 s rather than 0.5 s. The result of these differences is that participants did not pay attention to the stimulus after giving their initial choice or click response. This is evidenced by the lack of credible second-stage processing in this experiment (*SI Appendix*).

Finally, we examined how the accuracy of the confidence ratings changed as a result of this interference. To this end, we coded whether the confidence rating fell on the correct side of the scale relative to the actual left/right motion direction. In the choice and no-choice conditions, confidence ratings were on the correct side of the scale in 76.36% and 76.25% of cases, respectively. The accuracy of the confidence ratings in these conditions was credibly the same when we fit each one with a one-parameter Bernoulli distribution ($M_{\text{diff}} = 0.11\%$; 95% HDI $[-0.04\%, 0.20\%]$). The difference between the average confidence ratings and confidence accuracy is called bias, and it measures how well calibrated confidence ratings are to the proportion of times the target event actually occurs. The average bias statistic was 7.66, implying mild overconfidence (95% HDI $[-2.09, 17.66]$). Focusing on the interference effect, we found that overconfidence was lower, and thus, confidence was better calibrated in the choice condition than in the no-choice condition (8.20 vs. 7.13; $M_{\text{diff}} = 1.07$; 95% HDI $[0.29, 1.85]$) (for a similar result, see also ref. 21).

Direct Comparison of QRW and MRW

The interference effect of choice on subsequent confidence provides empirical support for a QRW theory of evidence accumulation over an MRW theory. However, the question remains if the QRW can provide a parsimonious account of the choice and confidence data. Therefore, we compared the QRW to a matched MRW using Bayesian model comparison methods. Both models used drift, diffusion, starting point variability, and attenuation parameters. Versions of the MRW with these parameters or more restricted ones (e.g., without attenuation) have been shown to account well for choice, response time, and confidence data, so superior performance would indicate that the QRW is a particularly viable model (2, 4).

Below we describe each model in mathematical detail (see also *SI Appendix*, Fig. S3, for a visual walk-through). In line with the established mathematical principles governing both the MRW and QRW theories, each one updates the state following a choice at time t_1 to produce a conditioned state that is consistent with the observed choice—for quantum theory, this is referred to as Lüder's rule. However, the two models differ with respect to the effect of this conditioning on the marginal distribution of confidence ratings. As our proof shows, the Markov model obeys the law of total probability, so that after pooling across choices the effect of conditioning on the choice completely disappears as if no choices were made. This is because the choice does not change the location of the evidence, only the information an external observer has about it. In contrast, the QRW violates the law of total probability because choice interacts with later evidence accumulation, making pooled confidence ratings after choice diverge from the no-choice case. This is because a definite state consistent with the choice is created, and subsequent dynamics are applied to the revised state, thereby producing the interference effect.

MRW. The MRW used $m = 103$ evidence states $x \in \{-1,0, \ldots 101\}$. This state space allowed us to assume that states $x = 0,1, \ldots 100$ corresponded directly with the $n = 101$ confidence ratings (0, 1, … 100%). The two boundary states (−1,101) served as reflecting boundaries that restricted the process to the range of the confidence scale, and these states were mapped onto confidence ratings of 0 and 100%, respectively. Using 103 states produces a Markov process that closely approximates a continuous state process, and increasing the number of states by refining the state space produces practically the same predictions.

According to the MRW, a decision-maker is in exactly one evidence state at any given time. However, the decision-maker's state is unknown to the observer, and a probability distribution across evidence states is therefore used to represent the state. This

Table 1. Summary of model comparison and statistical effects

Participant	Interference*	Second-stage processing†	Log Bayes factor
1	−0.18 [−0.26, −0.11]‡	0.12 [0.08, 0.18]‡	212
2	−0.15 [−0.23, −0.07]‡	0.08 [0.03, 0.14]‡	41
3	−0.15 [−0.22, −0.07]‡	0.01 [−0.04, 0.06]	−131
4	−0.14 [−0.23, −0.07]‡	0.10 [0.04, 0.15]‡	190
5	−0.11 [−0.19, −0.04]‡	0.07 [0.02, 0.13]‡	837
6	−0.08 [−0.16, −0.01]‡	0.13 [0.07, 0.18]‡	223
7	−0.07 [−0.15, 0.01]	−0.01 [−0.07, 0.05]	−148
8	−0.05 [−0.14, 0.02]	0.04 [−0.08, 0.10]	339
9	−0.01 [−0.09, 0.07]	−0.02 [−0.06, 0.04]	150
Group level	−0.11 [−0.18, −0.04]‡	0.06 [0.01, 0.12]‡	1,713

*Mean posterior coefficient and 95% HDI for main effect of the choice manipulation on half-scale confidence.
†Mean posterior coefficient and 95% HDI for the interaction between coherence and second stage processing time on full-scale confidence.
‡The 95% HDI excluded zero.

distribution is defined by a mixed state vector $\phi(t)$ of dimension $m \times 1$, which gives the probability of being in state x at time t,

$$Pr(x|t) = \phi_x(t). \quad [1]$$

The probability distribution $\phi(0)$ specifies the decision-maker's initial state, which is set as a uniform distribution centered on $x = 50$. The width w is a free parameter indexing trial-by-trial variability in the initial state.

As the decision-maker considers information, the process moves from state to state. An $m \times m$ transition matrix $\mathbf{P}$ specifies the probability that the process moves from one state to another after some period, so that the probability distribution over evidence states after time t is

$$\phi(t) = \mathbf{P}(t) \cdot \phi(0). \quad [2]$$

Choice probability and confidence are determined as follows. Define a response operator M_R, which is a diagonal matrix with 0.5 located in the row for confidence level 50, ones located in rows for confidence levels 51 through 101, and zeros otherwise. The probability of choosing right at time t_1, denoted $p(R|t_1)$, equals the sum of the projection $\mathbf{M}_R \cdot \phi(t_1)$. The probability of choosing left at time t_1 is $1 - p(R|t_1)$. If right motion is chosen, then this provides information on the location of the evidence (e.g., evidence is at or above state 50), and the probability distribution over the states is updated to $\phi(t_1|R) = \frac{\mathbf{M}_R \cdot \phi(t_1)}{p(R|t_1)}$. Note that if a person were to choose left motion, the response operator $\mathbf{M}_R$ would be replaced by $\mathbf{M}_L$; the two are identical except that the 1 and 0 entries along the main diagonal are flipped.

For confidence ratings, define $\mathbf{M}_y$ as a diagonal matrix with 1 located in the row(s) corresponding to confidence y and zeros otherwise. In the choice condition, the probability of choosing confidence level y at time t_2 following a right motion choice then equals the sum of the projection $\mathbf{M}_y \cdot \mathbf{P}(t_2) \cdot \phi(t_1|R)$. In the no-choice condition, the probability of choosing confidence level y at time t_2 equals the sum of the projection $\mathbf{M}_y \cdot \phi(t_2)$.

The transition matrix is constructed from an $m \times m$ intensity matrix $\mathbf{Q}$ using the Kolmogorov forward equation so that

$$\mathbf{P}(t) = \exp(\mathbf{Q}t\gamma), \quad [3]$$

where exp is the matrix exponential function and γ is a parameter describing the proportion of time spent processing information up to time t. Consistent with recent work in modeling postdecisional processing (15), this was set to $\gamma = 1$ during the first stage of processing (t_0 to t_1) but was free to vary during the second stage to account for attenuation in incoming information following the first response.

The entries $q_{j,k}$ of the intensity matrix are

$$q_{j,j} = -\sigma^2, \quad [4a]$$

$$q_{j-1,j} = \frac{1}{2}\left(\sigma^2 - \delta\right), \quad [4b]$$

$$q_{j+1,j} = \frac{1}{2}\left(\sigma^2 + \delta\right). \quad [4c]$$

This definition of the intensity matrix was chosen so that the discrete state Markov process closely approximates a continuous state Wiener diffusion process (8). The drift rate δ determines the probability that the process steps toward the true dot motion direction. We scaled the drift rate directly from the percentage of coherently c moving dots so that

$$\delta = \mu \cdot c. \quad [5]$$

If the dots are moving left, c is negative. The parameter μ is a free parameter indexing sensitivity to the coherence. The parameter σ^2 is a diffusion rate controlling the dispersion of the process. This MRW operates on a finite state space, so we set the states $x = -1$ and $x = 101$ as reflecting boundaries to allow the process to continue its evolution after it reaches the finite limits, $-q_{1,1} = q_{1,2} = \sigma^2$ and $q_{102,103} = -q_{103,103} = \sigma^2$.

QRW. The QRW also used $m = 103$ evidence states as in the MRW, similarly assuming that states $x = 0,1, \ldots 100$ corresponded directly with the 101 confidence ratings and that states $x = -1$ and $x = 101$ were reflecting boundaries which mapped onto confidence ratings of 0 and 100%.

According to the QRW, a decision-maker is not necessarily in any one evidence state at any given time. This uncertainty on the part of the decision-maker is modeled with a superposition state vector $\psi(t)$ of size $m \times 1$, which gives the probability amplitude at the xth evidence level at time t. The probability of observing state x at time t is the squared length of the amplitude in the corresponding row:

$$Pr(x|t) = |\psi_x(t)|^2. \quad [6]$$

The state vector $\psi(0)$ specifies the initial superposed evidence state. We set the probability amplitudes across these states to be uniformly and symmetrically distributed around $x = 50$. The width w of this distribution is a free parameter representing initial uncertainty.

As information is processed, the superposition state drifts over time until a response is elicited. The $m \times m$ unitary matrix operator $\mathbf{U}$ evolves the amplitudes over time, so that

$$\psi(t) = \mathbf{U}(t) \cdot \psi(0). \quad [7]$$

Choice probability and confidence are determined as follows. We define $\mathbf{M}_R$ in a similar manner as in the MRW. It is a diagonal matrix with $\frac{1}{\sqrt{2}}$ in the row for confidence level 50, ones located in rows for confidence levels 51 through 101, and zeros otherwise. The probability of choosing right at time t_1, denoted $Pr(R|t_1)$, equals the squared length of the projection $\mathbf{M}_R \cdot \psi(t_1)$. The probability of choosing left is $1 - Pr(R|t_1)$. If right motion is chosen, the superposition state is projected onto the corresponding evidence levels, and the probability amplitude is updated to $\psi(t_1|R) = \frac{M_R \cdot \psi(t_1)}{\sqrt{Pr(R|t_1)}}$. If left motion is chosen, $\mathbf{M}_R$ is replaced by $\mathbf{M}_L$; the two are identical except that the 1 and 0 entries along the main diagonal are flipped.

Subsequent processing starts from this new state so that in the choice condition the probability of choosing confidence level y at time t_2 after choosing right then equals the squared length of the projection $\mathbf{M}_y \cdot \mathbf{U}(t_2) \cdot \psi(t_1|R)$. In the no-choice condition, no projection is done at t_1, and the probability of choosing confidence level y at time t_2 equals the squared length of the projection $\mathbf{M}_y \cdot \psi(t_2)$.

The unitary matrix is constructed from a Hamiltonian matrix $\mathbf{H}$ using the Schrödinger equation so that

$$\mathbf{U}(t) = \exp(-it\mathbf{H}\gamma). \quad [8]$$

The attenuation parameter γ operates in the same way as in the MRW. The entries $h_{j,k}$ of the Hamiltonian matrix are

$$h_{j,j} = \delta \cdot j/m, \quad [9a]$$

$$h_{j-1,j} = h_{j+1,j} = \sigma^2. \quad [9b]$$

This definition of the Hamiltonian matrix was chosen so that the discrete state quantum process closely approximates the continuous state Schrödinger process (9). The δ and σ^2 parameters of the QRW have a similar effect as their counterparts in the MRW but function differently. The diffusion coefficient σ^2 controls the rate at which amplitude flows out of the states. The drift rate δ determines the rate at which probability amplitude flows in. The drift rate δ was set to be a multiplicative function of coherence

(Eq. **5**). [Eq. **9** is a linear potential function in the diagonal of the Hamiltonian (multiplying drift by the state index) so there is a constant positive force pushing evidence toward the correct direction. However, other potential functions (e.g., quadratic) should be investigated in the future.]

The interference effect arises because the amplitudes in states 0–50 interact with those in 50–100 in the no-choice condition, pushing each other outward toward more extreme evidence states. This pressure is not present in the choice condition, leading to less extreme evidence and hence confidence ratings. One consequence of these less extreme confidence ratings is less overconfidence in the choice condition.

Model Comparison. Each model has four free parameters: a parameter that sets the drift as a scalar function of motion direction coherence (μ), a diffusion parameter (σ^2), a second-stage attenuation parameter that dampens of the rate of incoming information after making a choice (γ), and a parameter that determines the width of the initial state distribution (starting point variability) (w) (*SI Appendix*, Table S3). Non-decision time parameters, accounting for components of the response time exogenous to the evidence accumulation process, had limited influence on model fits and were dropped in order to facilitate model estimation.

The models were compared at the individual level: for each participant and each model, four parameters were used to account for 2,688 trials across 24 experimental conditions. Despite having the same number of parameters, the QRW may be functionally more complex, allowing it to produce good fits to the data without necessarily bearing any relationship to the underlying process. To account for this, we compared the Bayes factor between the two models for each participant (22).

The Bayes factor was calculated using a fine-grid approximation across all possible combinations of the four parameters to compute the likelihood function and uniform priors over their values. The results are summarized in Table 1; the log Bayes factor indicates the log odds of the QRW model over the MRW given the data (see *SI Appendix*, Tables S4 and S5, for the maximum likelihoods and parameter estimates).

The Bayes factor for seven out of nine participants and the group level factor decisively favored the QRW (maximum likelihoods yield the same conclusion). Participant 7 did not show second-stage processing or an interference effect, so the MRW may well describe the behavior of this participant. Participant 3 was unable to distinguish between dot motion directions in many conditions, which caused difficulty in fitting both models (*SI Appendix*, Fig. S4). Future model development incorporating methods for mapping evidence to confidence (e.g., using only 0/10/20% or 0/50/100% ratings) could potentially improve fits, but this does not affect interference so we favor simpler, more parsimonious models here.

Fig. 3 illustrates the fit of each model to the choice proportions for each coherence condition and the distribution of confidence in the choice and no-choice conditions for one participant and coherence level [all participants across conditions are given in *SI Appendix*, Fig. S4 (see also *SI Appendix*, Figs. S5 and S6)]. There are several reasons that the QRW gives a better account of the data than the MRW. First, the MRW predicts identical marginal distributions of confidence ratings between choice and no-choice conditions, whereas the quantum model picks up the slight rightward shift of these ratings in the no-choice condition; this phenomenon is the interference effect we described (see *SI Appendix*, Fig. S6; the QRW posterior predictions yield a group mean shift in confidence of +0.66%, compared to +1.19% in the data). Second, the QRW was often better able to simultaneously capture choices along with confidence ratings across the various conditions, whereas the MRW often had to sacrifice or compromise between the two. Notably, the MRW underestimated choice proportions because higher diffusion more accurately captured confidence distributions but at the cost of predicting lower choice accuracy. Finally, the observed confidence distributions are frequently multimodal and discontinuous. The MRW again does not account for these properties. By contrast, the QRW accounts for all of these characteristics in a parsimonious way, operating only on its first principles to earn a superior Bayes factor.

Although this MRW and similar versions have been used to model a wide range of choice and judgment data, it may struggle to account for this data simply because it cannot account for the interference effect. To examine this possibility, we tested a second model—the MRW-E—which assumes that additional evidence may have been accumulated in the no-choice condition, producing more extreme confidence ratings and thus an interference effect. Despite the added ability to produce interference, the QRW still outperformed the MRW-E. The Bayes factor for seven out of nine participants and the group level factor again decisively favored the QRW over the MRW-E. In comparison with the MRW, the MRW-E provides a largely equivalent or often poorer fit in terms of Bayes factors (*SI Appendix*, Table S6 and Fig. S7). Part of the reason the MRW-E does poorly, in addition to the characteristics it inherits from the MRW, is that it assumes more evidence is accumulated in the no-choice condition producing a

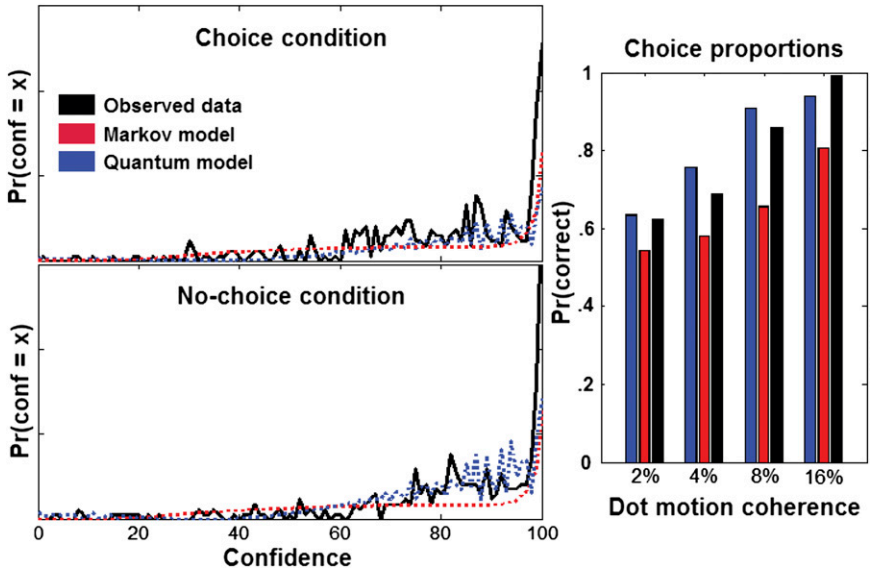

Fig. 3. Data and model fits for participant 4 with coherence level 8%.

change in the accuracy of the confidence ratings as well as the mean shift in confidence. Recall, however, that there is no credible change in the accuracy of the confidence ratings in the data.

Discussion

In this paper, we have developed a model of evidence accumulation during judgment and decision-making based on quantum random walk theory. The QRW represents a point of departure in modeling evidence accumulation from the more typical classical probability approach. In the classical case, evidence evolves over time, but judgments and decisions are simply read out from an existing state without changing the internal state of evidence. In the quantum case, evidence also evolves over time, but judgments and decisions are measurements that create a new definite state from an indefinite (superposition) state. This quantum perspective reconceptualizes how we model uncertainty and formalizes a long-held hypothesis that judgments and decisions create rather than reveal preferences and beliefs. The different approaches make competing a priori predictions for the effect of sequences of responses, and we have shown strong empirical support for the quantum prediction that choices interfere with subsequent confidence judgments. Moreover, we have shown for the first time to our knowledge that the QRW is a viable competitor to the MRW in quantitatively fitting choice and confidence distributions. Note that the QRW can also account for response time distributions (8) and can outperform Markov models in this area as well (10).

A pertinent question is whether the MRW can be adapted to account for the phenomena we observed. This is certainly possible but may prove difficult: as we have shown, our results provide several constraints on potential adaptations. The interference effect itself is a strong constraint: many versions of the MRW that commonly give good accounts of choice and confidence data do not predict any interference.

A second constraint is how the interference effect occurred. In particular, confidence was less extreme following a choice. This poses a problem for explanations like the confirmation bias, where people focus on evidence that justifies their decision after making a choice, meaning they should be more confident in the choice condition (23, 24). Moreover, confidence accuracy also did not change. This poses a problem for models like the MRW-E that assume different amounts of processing between the choice and no-choice conditions.

A third constraint is that the interference effect only occurred when there was second-stage processing. This result poses problems for explanations based on differences in the mapping of evidence onto confidence (25) and explanations assuming that the act of making a choice introduces error into the cognitive system. Both explanations would fail to explain why choice alone (without second-stage processing) does not interfere with confidence. Alternatively, on some trials during the choice condition, participants reversed their initial choice (14) and could have reported unexpectedly low confidence on these trials, producing the interference effect. However, reversals during the choice condition happened infrequently (6.1%), and confidence on reversal trials was only slightly lower than on consistent trials. We discuss this and other alternative models in more detail in *SI Appendix*, section F.

Although an alternative MRW may be found to account for our results, this does not diminish the QRW's significance in highlighting and challenging important assumptions regarding the judgment and decision-making process. In this paper, we have shown that a common assumption of cognitive and neural theories of decision-making—the read-out assumption—is violated even in a simple perceptual task. An interference effect occurred when participants were asked to make a decision about the leftward or rightward motion of a stimulus. Specifically, their subsequent confidence estimates were more conservative than when no earlier decision was made, and they were consequently less overconfident. This result, along with quantitatively superior model fits, lends strong support to the modeling of choice and confidence as a quantum random walk process, a model which describes decision-making as a constructive process wherein a definite state is created from an indefinite superposition. In addition to the cognitive implications, a QRW model of evidence accumulation potentially sidesteps the problem of how a group of neurons can produce observed behavior that is consistent with a single evidence accumulation trajectory (26). The QRW suggests that the mismatch might lie in the cognitive representation of evidence accumulation: instead of treating evidence accumulation as a single trajectory, it may be more accurate to conceptualize it as a wavelike superposition state. In fact, populations of interacting neurons processing evidence in parallel can give rise to a quantum random walk like the one presented here (10), and similar population coding models would certainly be capable of carrying out the necessary operations (27). Hence, quantum random walk theory provides a previously unexamined perspective on the nature of the evidence accumulation process that underlies both cognitive and neural theories of decision-making.

ACKNOWLEDGMENTS. This work was supported by grants from the National Science Foundation (NSF) (0955140) (to T.J.P.) and Air Force Office of Scientific Research (FA9550-12-1-0397) (to J.R.B.). P.D.K. was supported by a graduate fellowship from the NSF (1424871).

1. Gold JI, Shadlen MN (2007) The neural basis of decision making. *Annu Rev Neurosci* 30:535–574.
2. Ratcliff R, Smith PL (2004) A comparison of sequential sampling models for two-choice reaction time. *Psychol Rev* 111(2):333–367.
3. Bogacz R, Brown E, Moehlis J, Holmes P, Cohen JD (2006) The physics of optimal decision making: A formal analysis of models of performance in two-alternative forced-choice tasks. *Psychol Rev* 113(4):700–765.
4. Pleskac TJ, Busemeyer JR (2010) Two-stage dynamic signal detection: A theory of choice, decision time, and confidence. *Psychol Rev* 117(3):864–901.
5. Hanes DP, Schall JD (1996) Neural control of voluntary movement initiation. *Science* 274(5286):427–430.
6. Shadlen MN, Newsome WT (2001) Neural basis of a perceptual decision in the parietal cortex (area LIP) of the rhesus monkey. *J Neurophysiol* 86(4):1916–1936.
7. Lichtenstein S, Slovic P, eds (2006) *The Construction of Preference* (Cambridge Univ Press, Cambridge, UK).
8. Busemeyer JR, Wang Z, Townsend JT (2006) Quantum dynamics of human decision-making. *J Math Psychol* 50(3):220–241.
9. Feynman RP, Leighton RB, Sands M (2013) *The Feynman Lectures on Physics, Desktop Edition* (Basic Books, New York), Vol I.
10. Fuss IG, Navarro DJ (2013) Open parallel cooperative and competitive decision processes: A potential provenance for quantum probability decision models. *Top Cogn Sci* 5(4):818–843.
11. Kempe J (2003) Quantum random walks: An introductory overview. *Contemp Phys* 44(4):307–327.
12. Ma WJ, Beck JM, Latham PE, Pouget A (2006) Bayesian inference with probabilistic population codes. *Nat Neurosci* 9(11):1432–1438.
13. Busemeyer JR, Bruza P (2012) *Quantum Models of Cognition and Decision* (Cambridge Univ Press, Cambridge, UK).
14. Resulaj A, Kiani R, Wolpert DM, Shadlen MN (2009) Changes of mind in decision-making. *Nature* 461(7261):263–266.
15. Yu S, Pleskac TJ, Zeigenfuse MD (2015) Dynamics of postdecisional processing of confidence. *J Exp Psychol Gen* 144(2):489–510.
16. Busemeyer JR, Townsend JT (1993) Decision field theory: A dynamic-cognitive approach to decision making in an uncertain environment. *Psychol Rev* 100(3):432–459.
17. Usher M, McClelland JL (2001) The time course of perceptual choice: The leaky, competing accumulator model. *Psychol Rev* 108(3):550–592.
18. Ratcliff R, Rouder JN (1998) Modeling response times for two-choice decisions. *Psychol Sci* 9(5):347–356.
19. Ball K, Sekuler R (1987) Direction-specific improvement in motion discrimination. *Vision Res* 27(6):953–965.
20. Kruschke J (2010) *Doing Bayesian Data Analysis: A Tutorial Introduction with R* (Academic, Waltham, MA).
21. Sniezek JA, Paese PW, Switzer FS, III (1990) The effect of choosing on confidence in choice. *Organ Behav Hum Decis Process* 46(2):264–282.
22. Kass RE, Raftery AE (1995) Bayes factors. *J Am Stat Assoc* 90(430):773–795.
23. Koriat A, Lichtenstein S, Fischhoff B (1980) Reasons for confidence. *J Exp Psychol Learn Mem Cogn* 6(2):107–118.
24. Zylberberg A, Barttfeld P, Sigman M (2012) The construction of confidence in a perceptual decision. *Front Integr Neurosci* 6:79.
25. Green DM, Swets JA (1966) *Signal Detection Theory and Psychophysics* (Wiley, New York), Vol 1.
26. Zandbelt B, Purcell BA, Palmeri TJ, Logan GD, Schall JD (2014) Response times from ensembles of accumulators. *Proc Natl Acad Sci USA* 111(7):2848–2853.
27. Pouget A, Dayan P, Zemel R (2000) Information processing with population codes. *Nat Rev Neurosci* 1(2):125–132.

Interference effects of choice on confidence: Quantum characteristics of evidence accumulation

Peter D. Kvam, Timothy J. Pleskac, Shuli Yu, & Jerome R. Busemeyer

Supplementary Information

Table of Contents:

Appendix A – Methods

Participants. We recruited 9 undergraduate and graduate students (7 female, 2 male; 19-27 years old) from a pool of people who had responded to flyers posted around the Michigan State University campus and East Lansing community. The flyers advertised for people who

wanted to participate in paid studies on judgment and decision making. An additional 2 participants did not return after the first session, so they were excluded from further analyses. Participants were paid $8 per hour and could receive up to $5 more based on how many points they earned divided by the number of points it was possible to earn.

Random dot motion (RDM) stimulus. The motion display was similar to that used in previous neuropsychological studies [1,2,3]. The RDM stimulus consisted of a field of white moving dots on a black background, presented on a circular aperture of 10° diameter. There were three interleaved sets of dots such that each set was re-plotted three video frames later, On each iteration of the same set, some percentage of the dots were displaced by .25° to produce apparent motion at 5°/s velocity, while the remaining dots were plotted at random locations. The probability that a specific dot was displayed in motion is termed motion coherence. We used four levels of motion coherence: 2%, 4%, 8%, and 16%. The task was programmed using the Psychtoolbox extensions [4,5].

RDM practice (Session 1). The purpose of this task was to train participants to make timely responses immediately after hearing an auditory cue. During a given trial, a RDM stimulus appeared on screen and participants pressed either the left mouse button (←) or the right button (→) to indicate which direction they believed a majority of the dots were moving. First, they did 5 trials where they could make their decision response at any time. They also did 10 trials of prompted decision training, in which they were instructed to enter their decision immediately after a 400 Hz beep that took place at either 0.5 or 1.0 s after stimulus onset. After each trial, participants were given feedback about their decision accuracy and timing (responses more than 500ms after the beep were met with a prompt to try to respond faster).

Confidence scale practice (Session 1). Participants completed a series of trials to

become familiar with entering a confidence rating with the mouse. During a given trial a fixation display was shown for 500ms, then a percentage value (e.g., 9%) appeared just below the center of the screen. The semicircular confidence rating scale (see Fig. 2), used to control for the distance traveled to select a confidence rating with the mouse, also appeared onscreen above the percentage value. Participants moved the cursor with the mouse from the center of the screen to the appropriate point on the scale to match the value as quickly and accurately as possible. The value of the confidence rating was randomized and participants continued until they achieved at least 10 answers that were within 2 percentage points of the correct number.

In addition, participants saw 15 trials of the random dot motion task with no mouse click element included – 5 trials in which they could simply enter a confidence rating when they saw fit, and 10 trials in which they were prompted with a beep to make a confidence response. This 400 Hz beep occurred at 1.0 or 2.0 s following stimulus onset.

RDM direction discrimination task. The time course of a trial for the choice and no-choice conditions is shown at the top and bottom (respectively) of Figure 2. Participants would start each trial of the task by clicking on a small fixation shape, which was either a circle (during choice trials) or a square (during no-choice trials). Once clicked (centering the mouse cursor), it would persist for 0.3 s before the RDM stimulus came on-screen and the mouse cursor was removed from the screen. In the choice condition, participants were cued via a low frequency beep (400 Hz) at 0.5 s from stimulus onset to choose which direction the majority of the dots were moving, left or right. Participants recorded their choice by pressing either the left or right mouse button. In the no-choice condition, participants were cued via a high frequency beep (800 Hz) at 0.5 s from stimulus onset to click either the left or right mouse button. The mouse button was specified at the beginning of that block of trials (the left or right mouse button specification

alternated between blocks). A different frequency beep was used to minimize any confusion participants experienced between the two conditions.

After participants made their choice or clicked the button, a semi-circular confidence scale (from 0 to 100%, with major demarcations at 10 point intervals and minor demarcations at every 1; see main text, Fig. 2) appeared over the upper half of the field of dots. The confidence scale was in terms of the confidence the dots were moving right, i.e., confidence of 0% indicated participants were certain the dots were moving left and a confidence of 100% indicated participants were certain the dots were moving right. Confidence judgments were cued at 0.05, 0.75, or 1.5 s after the initial choice or click response was entered.

Procedure. During the first session, participants first received a presentation describing the task that they were about to do. This included a description of all conditions and response modes. These directions were repeated on-screen during the training described above, which enabled them to practice making decisions and using the confidence scale. In addition, at the end of their first session, they saw a plot comparing dot coherence against their choice accuracy along with a Weibull fit line. We explained this plot to participants, noting that it should be an increasing function (it was for all participants in this experiment).

At the beginning of each session, in addition to the training trials described in the sections above, participants would do 10 trials each of the choice and no-choice conditions. These were organized into 4 blocks (2 choice, 2 no-choice) so participants could get accustomed to the task once again before we collected new data.

The different conditions were organized into blocks of trials such that each block contained 2 iterations of each of the 4 levels of dot coherence (2 / 4 / 8 / 16%) crossed with each of the 3 levels of the duration of the second stage of processing (0.05 / 0.75 / 1.5 s) for a total of

24 trials / block. Half of these blocks were choice blocks, where the pre-trial fixation was a red circle (see main text Fig. 2) with a 400 Hz beep to prompt a choice response after 500ms of stimulus presentation. The other half were no-choice blocks, where the pre-trial fixation was a red square and a 800Hz beep prompted them to click the right button on half of the no-choice blocks and the left button on the other half of the no-choice blocks (i.e. 2/4 blocks were choice, 1/4 were click-right, 1/4 were click-left). They were informed prior to the start of each block as to which type it would be. Mean response times after t_1 for the choice condition were 0.548 (Median = 0.370, SD = 0.625) s for the choice condition and 0.383 (Median = 0.298, SD = 0.333) s for the no-choice condition. After t_2, confidence response times were 0.767 (Median = 0. 863, SD = 0.392) s for the choice condition and 0.767 (Median = 0.871, SD = 0.391) s for the no-choice condition.

After each trial, participants received feedback about whether their click was correct (whether their choice was correct on choice trials, or whether they clicked in the requested direction on the no-choice trials) as well as how many points they received for their confidence response. The amount of points participants received from their confidence rating was determined using a linear transformation of the Brier scoring rule [6]:

$$\text{Score} = 100 * [c - (conf / 100)]^2.$$

The variable *c* indicates the correct answer (0 for left, 1 for right) and *conf* indicates their response on the absolute scale (0 for certain left, 100 for certain right). The Brier scoring rule is a strictly proper scoring rule, meaning that the optimal strategy on the part of the participant is to provide a probability estimate that matches one's true subjective probabilities.

Appendix B – Regression Analyses

All regression analyses used hierarchical Bayesian linear models that included all possible interactions between predictors ([7], chapter 14). Vague priors were used for each parameter so as to let the data have maximal influence on the posterior estimates. We report the mean estimate of the slope parameter corresponding to a predictor (*b*) as well as the interval that contains the 95% most credible values for this parameter (Highest Density Interval / HDI). In practice, these highest density intervals tended to be fairly similar to the estimates one would obtain for a 95% confidence interval, but were slightly stricter (were closer to 0 than a corresponding classical confidence interval).

Linear regression analyses all used MATLAB, JAGS, and matjags to fit the model. Each analysis was estimated using 8 parallel chains. Each chain was comprised of 1000 burn-in steps (unrecorded samples to allow the chain to reach the reasonable parameter space) and 10,000 samples. Preliminary analyses confirmed that all chains converged. Each of the analyses reported in the paper are described individually below:

Accuracy by coherence and second stage duration. Choice accuracy in the choice condition was predicted by coherence level, the duration of the second stage, and their interaction. A logit link function was used for this analysis.

Confidence by coherence, second stage duration, choice/no-choice. In order to gauge how confidence changed over the different conditions, we transformed confidence responses so that they reflected how sure a participant was of the direction of dot motion, i.e. collapsed across directions in which they could respond. This resulted in confidence responses (*y)* ranging from 50% (unsure of motion direction) to 100% (certain of motion direction) based on raw responses

(r) from the 0 (certain left) to 100 (certain right) scale. The cumulative distributions of confidence for each individual on this scale is shown in Figure S1.

$$y = \begin{cases} 100 - r, & r < 50 \\ r, & r \geq 50 \end{cases}$$

Coherence, duration of second stage, and the choice / no-choice manipulation were used as predictors. Fig. S2 below plots how mean confidence changes over each of these manipulations. Table S1 lists the mean group level coefficients and their HDI's for each of the experimental factors: IJT duration, degree of motion coherence, and the choice/no choice manipulation.

Confidence on full scale by coherence and duration of second stage. The interference effect relies on second stage processing in order to appear – there should be some change in confidence over time after t_1 and the magnitude of this change should depend on the coherence of the stimuli, which implies an interaction between the duration of the second stage and dot motion coherence. During this second stage, we assume information about the state of the stimulus continues to be sampled and accumulated [8]. This suggests that additional information should lead to higher levels of confidence when accumulated evidence already favors the correct answer at t_1. However, when accumulated evidence reflects the incorrect answer at t_1, new information should conflict with the existing information, on average decreasing a person's confidence [8,9]. These conflicting forces reduce the effect of second stage processing time on confidence when it is coded on a half-scale, resulting in a null effect of second stage processing time x coherence as reported in Table S1. However, the effect of second stage processing can be much better seen if confidence ratings discriminate between correct and incorrect responses. To

do this, the confidence ratings were transformed from the raw scale (r) framed in terms of the state of the stimulus to a full scale (s), in terms of the true direction:

$$s = \begin{cases} 100 - r, & \textit{if the dots were moving left} \\ r, & \textit{if the dots were moving right} \end{cases}$$

That is, a raw scale rating of $r = 40$ when the dots were moving left would mean they were $s = 60\%$ certain in the correct direction; and a raw scale rating of $r = 60$ when the dots were moving to the right would also mean they were $s = 60\%$ certain in the correct direction. We submitted these transformed confidence ratings to a Bayesian hierarchical regression where the predictors were coherence, second stage processing time, and their interaction. We report the interaction in the main text and Table S2 shows the effect of each.

Appendix C – Proofs

Recall that in the experiment, participants viewed a random dot motion stimulus and reported a confidence rating in the direction of the moving dots at time t_2. On some trials, prior to the making a confidence rating, participants first chose which direction they thought the dots were moving at $t_1 = t_2 - t$. On other trials they made no choice and only clicked the mouse at t_1. Below, we show that the MRW predicts no difference in the marginal distributions of confidence ratings between these two conditions, and that the QRW predicts that the two distributions will not be identical. Note this proof is an adaptation of the proof in [10] (see Ch.8, p. 248).

For simplicity, we assume a 1:1 mapping of evidence states onto confidence, but these proofs hold for any consistent mapping of evidence onto confidence as well as for models with decay and drift rate variability.

Mathematical proof of non-interference in MRW. The MRW predicts that the marginal distribution of confidence ratings in the two conditions (choice and no choice) should be equal, $Pr(conf = y|t_2, choice) = Pr(conf = y|t_2, \ no\text{-}choice)$. To see this, we define three $m \times m$ state to response probability transition matrices. The first, $\mathbf{M}_{correct}$, is for choosing correctly and is filled with zeroes everywhere except for a series of ones along the main diagonal in rows corresponding to confidence levels 51-100 and a ½ at the row corresponding to confidence level 50. The second, $\mathbf{M}_{incorrect}$, is for choosing incorrectly. It is filled with zeroes everywhere except for ones along the main diagonal in rows representing levels 0-49 and a ½ at the row corresponding to confidence level 50. The third, $\mathbf{M}_y$, is used to give the probability of a confidence rating y and is entirely zeroes except for a one in cell corresponding to confidence rating y. It is important to note, however, that the proof shown below does *not* depend on these specifications for $\mathbf{M}_{correct}$ and $\mathbf{M}_{incorrect}$. The proof is valid for any $\mathbf{M}_{correct}$ and $\mathbf{M}_{incorrect}$ that have positive entries and satisfy the following completeness requirement $\mathbf{M}_{correct} + \mathbf{M}_{incorrect} = \mathrm{I}$, where I is the identity matrix. Thus the proof holds for a much more general class of measurements at choice than the specific model that we fit to the data. Finally, let $\mathbf{L}$ be a $1 \times m$ matrix filled with ones, which we use to sum the values across states.

In the choice condition, the probability of giving a particular confidence rating y at time t_2 after a choice (at t_1) is simply the marginal sum across correct and incorrect answers, which we can show is equivalent to the probability of giving confidence rating y at t_2 in the no-choice condition:

$$
\begin{aligned}
&\Pr(conf = y \mid t_2, choice) \\
&= \Pr(correct \text{ at } t_1 \cap conf = y \text{ at } t_2) + \Pr(incorrect \text{ at } t_1 \cap conf = y \text{ at } t_2) \\
&= \mathbf{L} \cdot [\mathbf{M}_y \cdot \mathbf{P}(t) \cdot \mathbf{M}_{correct} \cdot \mathbf{P}(t_1) \cdot \phi(0) + \mathbf{M}_y \cdot \mathbf{P}(t) \cdot \mathbf{M}_{incorrect} \cdot \mathbf{P}(t_1) \cdot \phi(0)] \\
&= \mathbf{L} \cdot \mathbf{M}_y \cdot \mathbf{P}(t) \cdot [\mathbf{M}_{correct} \cdot \mathbf{P}(t_1) \cdot \phi(0) + \mathbf{M}_{incorrect} \cdot \mathbf{P}(t_1) \cdot \phi(0)] \\
&= \mathbf{L} \cdot \mathbf{M}_y \cdot \mathbf{P}(t) \cdot \mathbf{I} \cdot \mathbf{P}(t_1) \cdot \phi(0) \\
&= \mathbf{L} \cdot \mathbf{M}_y \cdot \mathbf{P}(t + t_1) \cdot \phi(0) \\
&= \Pr(conf = y \mid t_2, no - choice)
\end{aligned}
$$

As we can see, the MRW must obey the law of total probability (in this context, this is called the Chapman – Kolmogorov equation) for every confidence level *y*, and therefore it predicts that the marginal distribution of confidence ratings between the choice and no-choice conditions should be identical. The same prediction holds when the transition matrix is non-stationary, as can be seen by replacing $\mathbf{P}(t)$ with $\mathbf{P}(t_i, t_j)$. Note the prediction does assume the initial state $\phi(0)$ is the same for both conditions. It also assumes that the transition matrices do not change across conditions; however, the transition matrices could change across time and the same conclusion would follow.

Mathematical proof of interference in QRW. To see the predicted violation of the law of total probability (i.e., the interference effect), we define three state-response amplitude transition matrices: $\mathbf{M}_{correct}$, $\mathbf{M}_{incorrect}$, and $\mathbf{M}_y$. These matrices are equivalent everywhere to the corresponding state probability transition matrices for the MRW described earlier, with the exception that there is a $\frac{1}{\sqrt{2}}$ placed in the row corresponding to confidence level 50 for $\mathbf{M}_{correct}$ and $\mathbf{M}_{incorrect}$. In the QRW, each of these matrices is a projection operator that collapses a vector onto the subspace spanned by the corresponding basis states. This means that when we take the

squared magnitude of each entry (element-wise), $\mathbf{M}_{correct} + \mathbf{M}_{incorrect} = \mathrm{I}$ (the combined correct and incorrect projection operators include all possible responses).

According to the QRW, in the choice condition, the marginal distribution of confidence ratings at t_2 following a choice at t_1 are as follows:

$$
\begin{aligned}
&\Pr(conf = y \mid t_2, choice) \\
&= \Pr(correct \text{ at } t_1 \cap conf = y \text{ at } t_2) + \Pr(incorrect \text{ at } t_1 \cap conf = y \text{ at } t_2) \\
&= \left\| \mathbf{M}_y \cdot \mathbf{U}(t) \cdot \mathbf{M}_{correct} \cdot \mathbf{U}(t_1) \cdot \psi(0) \right\|^2 + \left\| \mathbf{M}_y \cdot \mathbf{U}(t) \cdot \mathbf{M}_{incorrect} \cdot \mathbf{U}(t_1) \cdot \psi(0) \right\|^2 \\
&\neq \left\| \mathbf{M}_y \cdot \mathbf{U}(t) \cdot \mathbf{M}_{correct} \cdot \mathbf{U}(t_1) \cdot \psi(0) + \mathbf{M}_y \cdot \mathbf{U}(t) \cdot \mathbf{M}_{incorrect} \cdot \mathbf{U}(t_1) \cdot \psi(0) \right\|^2 \\
&= \left\| \mathbf{M}_y \cdot \mathbf{U}(t) \cdot \mathbf{I} \cdot \mathbf{U}(t_1) \cdot \psi(0) \right\|^2 \\
&= \left\| \mathbf{M}_y \cdot \mathbf{U}(t_1 + t) \cdot \psi(0) \right\|^2 \\
&= \Pr(conf = y \mid t_2, no - choice)
\end{aligned}
$$

As the inequality (line 4) demonstrates, the QRW does not obey the law of total probability, instead allowing for and predicting an interference effect where the marginal distributions of confidence ratings can be different between the choice and no-choice conditions. This effect occurs because making a choice changes the state of the system, impacting subsequent processing. However, it is important to note that for this violation to occur, the unitary operator $\mathbf{U}(t)$, corresponding to processing between t_1 and t_2, must be applied. Otherwise both conditions would simple reduce to the squared magnitude for one and the same amplitude, that is $\Pr(conf = y \mid t_2) = |\psi_y(t_2)|^2$.

Appendix D – Model Comparison

Each model used 4 parameters in order to fit the data: coherence multiplier μ, diffusion σ, time-dependent attenuation γ, and initial distribution width w. In order to obtain drift for each

coherence level, we multiply the drift coefficient by each coherence 2, 4, 8, 16%), giving 4 levels of drift for each drift parameter. Initially, we included parameters corresponding to non-decision and non-judgment time, but these were dropped because they drastically increased the computational demands of model fitting without substantially contributing to model performance.

Note that in the Markov model we present in the paper, we set the decision bounds to -1 and 101 and the step size Δ to 1, resulting in equations 4a-c and 5. However, to draw it closer to the typical Markov approximation of a Wiener diffusion model, which uses bounds of -1 and 1, one could set $\Delta = 1/51$ and begin the process at state 0. For each time they occur in the model description, we would then set $\sigma = \sigma \cdot \Delta$ ($\sigma^2 = \sigma^2 \cdot \Delta^2$) and $\mu = \mu \cdot \Delta$ ($\delta = \mu \cdot c \cdot \Delta$) (see [11]).

In order to fit the models and compute a Bayes factor between them, we took a grid of 21 drift, diffusion, and attenuation parameters and 51 initial distribution parameters and calculated the log of the multinomial function at each point in order to form a 21 x 21 x 21 x 51 grid approximation of the likelihood function:

$$\ln[Pr(D \mid Model)]$$

$$= \sum_{c=1}^{4}\sum_{i=1}^{3}\Bigg(n_{corr,c,i} \cdot \ln[\Pr(corr|Model, t_1, c, i)] + n_{incorr,c,i}$$

$$\cdot \ln[\Pr(incorr|Model, t_1, c, i)]$$

$$+ \left[\sum_{x=0}^{100} r_{choice,corr,c,i,x} \cdot \ln(\Pr[conf = x|Model, t_2, choice, corr, c, i])\right]$$

$$+ \left[\sum_{x=0}^{100} r_{choice,incorr,c,i,x} \cdot \ln(\Pr[conf = x|Model, t_2, choice, incorr, c, i])\right]$$

$$+ \left[\sum_{x=0}^{100} r_{no-\ choicec,i,x} \cdot \ln(\Pr[conf = x|Model, t_2, no - choice, c, i])\right]\Bigg)$$

The entries $n_{corr,c,i}$ and $n_{incorr,c,i}$ are the number of correct and incorrect choices, respectively, at t_1 in the choice condition for coherence level c =1 to 4 and second-stage processing time level i = 1 to 3. Pr(*corr* | *Model*, t_1, *c*,*i*) and Pr(*incorr* | *Model*, t_1, *c*,*i*) are the choice probabilities for correct and incorrect choices for model M at t_1 in coherence condition *c* and second-stage processing time level *i* (note that the predicted choice probabilities are the same for different levels of second-stage processing time, but we include these levels for completeness). The variables $r_{choice,\ corr,c,i,x}$, $r_{choice,\ incorr,c,i,x}$, and $r_{no\ choice,\ c,i,x}$, correspond to the number of confidence ratings at each confidence level *y* for each condition. Pr(*conf = y* | *Model*, t_2, *choice*, *corr*, *c*, *i*), Pr(*conf = y* | *Model*, t_2, *choice*, *incorr*, *c*, *i*), Pr(*conf = y* | *Model*, t_2, *no-choice*, *corr*, *c*, *i*), are the predicted probabilities of responding with confidence level y in the respective condition.

The parameters and a brief description of their function are given in Table S3. For the priors, a uniform distribution over these values was used, so each grid point had equal weight in calculating the posterior likelihood. The ranges of possible values are also given in Table S3. Note that the models use different ranges of parameters, as the scale for the two is not quite comparable (see [10]).

We used these log likelihoods and priors to calculate the log Bayes factor between the two models for each participant and for the overall group:

$$\ln\left[BF(\frac{QRW}{MRW}) \right] = \ln\left[\frac{\sum_n \Pr(D \mid QRW_n) \Pr(QRW_n)}{\sum_n \Pr(D \mid MRW_n) \Pr(MRW_n)} \right]$$

The indicator *n* is the n^{th} grid point for each model, $\Pr(D|Model_n)$ is the likelihood generated from the set of parameters at that grid point, and $\Pr(Model_n)$ is the prior probability of the model at that grid point. This term cancels out for the MRW / QRW comparison, as each model has uniform priors over the same number of grid points, but is important when considering the MRW-E because it uses more free parameters and the prior probability over each point is therefore lower. Note that the likelihood grid allows us to compute the maximum likelihood estimates for each model as well. These do not deviate much from the Bayes factors, indicating that the priors had little effect on the overall model comparison.

Note that in evaluating the Markov and quantum models, we used the full scale coded in terms of the true direction. Thus, states 51-101 correspond to correct responses, states -1-49 correspond to incorrect ones, and half of the time a 50 state was correct and the other half it was incorrect.

We present the resulting Bayes factors in in Table 1 in the main text, and the maximum log likelihoods and parameter values in Tables S4 and S5 respectively. The confidence distributions generated from these maximum likelihoods, collapsed across coherence levels and second stage processing times, are shown in Figures S4 and S7, and the misfit between the models by coherence level (but collapsed across second stage processing times) are plotted in Figure S5. These serve to illustrate the misfit in the MRW and QRW. Noticeably, the MRW performs worst at high coherence levels and tends to under-estimate the probability of responses in the 0-20 and 80-98 confidence range, illustrating its inability to capture the multimodal confidence distributions. In addition, it predicts more confidence responses at 100% than at nearby lower levels (80-99%). This is largely because spreading out predicted distributions would entail higher values of diffusion, reducing choice proportions when they are already substantially underestimated (see Figures S4 and S7).

Appendix E – Brief report of study without interference effect

In a different study, we also compared a choice condition to a no-choice condition. A total of 8 MSU students participated in 8 sessions (4680 trials) each, with training and blocking that was identical to the experiment reported above. The second-stage processing time delays were the same (0.05 / 0.75 / 1.5 s), and the choice / click manipulation was done in the same way, but an additional level of coherence was included, giving coherence levels of 2 / 4 / 8 / 16 / 32%. However, in this study we did not give feedback and used a longer duration for t_1. The 400 Hz/800 Hz beep for the choice / no-choice conditions was played at 0.8 s. With these changes, we found no evidence of second stage processing of information as indicated by an interaction between coherence and second-stage processing time predicting confidence judgments (b = .05; 95% HDI = [-.0.02, 0.12]). Other interactions with second-stage processing time similarly were

non-credible. There was also no effect of the choice/no-choice manipulation (i.e., interference effect) (b = 0.02; 95% HDI = [-0.01 0.05]). The distributions of confidence judgments were statistically indistinguishable. For instance, the mean confidence judgment in the choice condition was (M = 84.91; SD = 15.29) while in the click conditions these values were (M = 84.87; SD = 15.39). This pattern of results reveals that a choice at the first time point is not sufficient for the interference effect at the second time point. Rather, the interference effect requires both a choice and second stage processing (modeled with the application of the Schrödinger evolution operator in the quantum random walk model) for interference to appear (see earlier proof). We discuss the implications of this experiment more in the main text.

Appendix F – Alternative models

Summary of alternative models addressed by our results. As we discuss in the text, it is certainly possible that a MRW may be found to account for our results. However, our results provide several constraints on potential adaptations. Below we list 17 different versions of the MRW and review how different aspects of our data rule them out.

1. A basic MRW with drift, diffusion, and starting point variability parameters (nested within models 2 and 3)
2. A MRW including time-dependent attenuation and reflecting boundaries (nested within model 3)
3. A MRW which assumes additional processing before the click response is made in the no choice condition, along with time-dependent attenuation and reflecting boundaries.
4. Confirmation bias (sampling information in favor of chosen alternative)

5. Alternative models with information loss or noise insertion when a choice response is made (including MRW)
6. An MRW with an increased drift rate after choice
7. An MRW with a decreased drift rate after choice
8. An MRW with increased diffusion after choice
9. An MRW with decreased diffusion after choice
10. An MRW using category boundaries to bin confidence judgments (as in 2DSD [8]), including a version where criteria are shifted for choice vs no-choice to create an interference effect
11. A model with competing accumulators for confidence judgments (as in Ratcliff and Starns' RTCON [12,13]) where the accumulators change between choice and no-choice.
12. Explanations suggesting that more information is sampled in the no-choice condition after an initial response is made
13. An MRW with drift rate variability
14. An MRW with absorbing confidence boundaries
15. Explanations involving more information sampling in the choice condition, either before or after choice
16. Other methods of confidence binning
17. Lower confidence for incidences of choice-confidence conflict

Models 1, 2, 13, and 14 – the canonical Markov random walk models – can be ruled out by the mere presence of an interference effect, as we show in the proof in Appendix C. Models 4, 5, 6, 8, and 15 can be ruled out by the direction of the interference effect (more extreme confidence in

the no-choice condition), which was the opposite of what we and other researchers had predicted in advance of our results. Models 3-9, 12, and 16 predict different confidence accuracy (percentage of the time that confidence judgments fall on the correct side of the scale) between the choice and no-choice conditions, which was not the case (Choice = 76.36%, No-choice = 76.25%, Difference = 0.11%, 95% HDI = [-0.04%, 0.20%]), as well as an interaction between coherence level and the size of the interference effect, which was also not the case (from Table S1: b = 0.04, 95% HDI = [-0.04, 0.12]). Finally, models 1-5 and 10-16 fail to account for the finding that interference does not arise without second stage processing. Models 10, 11, and 16 additionally fail to account for interference without requiring additional assumptions, but they (or similar versions for the QRW) could perhaps be used to account for the individual variation in response mappings (e.g. using responses 0/50/100 [participant 5] versus 0/10/20/…/100. [participant 7] or the full scale [participant 2]).

Model 17 is somewhat more nuanced, suggesting that instances where participants gather sufficient evidence to reverse their decision (in the choice condition) should lead to lower confidence. There are two issues with this proposal. First, reversals in the choice condition are rare, constituting only 6.1% of choice trials. For reference, this means that relative to instances where evidence crossed sides of the confidence scale between t_1 and t_2 in the no-choice condition (which according to both models should be roughly as prevalent as the number of choice reversals), each reversal in the choice condition would have to be on average 16 points lower on the scale to create a 1% confidence difference between the conditions. This is extremely unlikely, especially given that mean confidence in cases of reversals was 82.5%, only slightly lower than the overall mean of 84.0% in the choice condition. Second, as might be expected, the rate of counter-decisional confidence estimates more than doubles across coherence levels (2%

coherence = 8.0% reversals, 4% coherence = 5.6% reversals, 8% coherence = 7.4% reversals, and 16% coherence = 3.7% reversals). This would mean that the interference effect size would interact with coherence, producing larger interference at lower coherence levels and a positive interaction between coherence and choice / no-choice, which was not found (see Table S1).

Markov random walk with extra processing in no-choice condition (MRW-E). The MRW model we used in the model comparison in the main text is a standard MRW which has been used extensively in the dynamic decision-making literature. However, it could be the case that its inferior fits are caused by its inability to create any interference effect between choice and no-choice conditions. One suggestion that has been raised is that participants actually process more information in the no-choice condition, as making a choice results in more "time out" from processing than making a click response. This corresponds to model 3 in the previous section. Note that this model actually predicts an interference effect in absence of second stage processing, a negative interaction between dot motion coherence and the choice / click manipulation on confidence, and higher confidence accuracy in the no-choice condition. In some cases, reflecting boundaries may interfere with the interaction between coherence and interference – however, in these cases we would expect 2- or 3-way interactions between interference, coherence, and second stage processing, none of which were substantiated (see Table S1). While none of these claims are supported by the data, we are unaware of any classical MRW that clears these empirical hurdles, so a model that can at least create an interference effect in the correct direction is a relatively good point of comparison.

In order to fit this model, we modified the MRW presented in the paper by including an additional free parameter ε, which adds an additional 0, 50, 100, 150, 200, 250, 300, or 350 ms of processing time to the no-choice condition. A value of $\varepsilon = 0$ gives the (nested) original MRW

presented in the paper, and larger values of ε create a progressively larger interference effect. However, this additional parameter comes at the cost of increased flexibility, which is penalized in the Bayes factor.

The result of the comparison between the original MRW and this modified MRW, which we refer to as MRW-E model for the epsilon parameter, is presented in Table S6. For participants 1, 4, 5, 7, 8, and 9, the best-fitting MRW-E model was actually the one with $\varepsilon = 0$, which corresponds to the nested MRW presented in detail in the main paper. Therefore, the Bayes factor favored the original MRW for these participants, as the additional parameter did not improve fits.

For the remaining participants, the best fitting ε value was 50 (50 ms of additional processing in the no-choice condition), with all other parameters similar to those of the original MRW. It still failed to improve the fit over the original MRW for one of these participants (participant 3), and while it improved fits for the other two (participants 2 and 6), the change in fit was too small to affect the comparison between the MRW and the QRW (Table S6). Therefore, adding this additional parameter to the MRW in order to introduce interference does not substantially affect the results or interpretation of the model comparison presented in the main text.

Given the relatively sparse differences between the MRW and MRW-E fits, it should perhaps not be surprising that the posterior fits are similar as well. These are shown in Figure S7. With only 50 ms of additional processing for half of the conditions for 3 participants, the predictions are essentially identical to the MRW predictions shown in Figure S4 – the rightward shift of no-choice conditions for participants 2, 3, and 6 is nearly imperceptible.

The inability of this model to account for the data comes down the same factors that hurt the MRW in the main paper – it could not account for the wavy or multimodal shape of the confidence distributions and it had to trade between fitting choice proportions and confidence distributions (e.g. it had higher diffusion values because this more accurately captured the distribution of confidence, even though it decreased choice proportions).

References

1. Shadlen, M. N., & Newsome, W. T. (2001). Neural basis of a perceptual decision in the parietal cortex (area LIP) of the rhesus monkey. *Journal of Neurophysiology, 86*(4), 1916–1936.
2. Liu, T., & Pleskac, T. J. (2011). Neural correlates of evidence accumulation in a perceptual decision task. *Journal of Neurophysiology*, *106*(5), 2383–2398. doi:10.1152/jn.00413.2011
3. Britten, K. H., Shadlen, M. N., Newsome, W. T., & Movshon, J. A. (1992). The analysis of visual motion: a comparison of neuronal and psychophysical performance. *The Journal of Neuroscience*, *12*(12), 4745–4765.
4. Brainard, D.H. (1997). The psychophysics toolbox. *Spatial Vision 10*, 433–436.
5. Kleiner, M., Brainard, D., Pelli, D., Ingling, A., Murray, R., & Broussard, C. (2007). What's new in Psychtoolbox-3. *Perception*, *36*(14), 1-1.
6. Brier, G. W. (1950). Verification of forecasts expressed in terms of probability. Monthly Weather Review, 78, 1–3.
7. Kruschke, J. (2010). *Doing Bayesian Data Analysis: A Tutorial Introduction with R.* Academic Press.
8. Pleskac, T. J., & Busemeyer, J. R. (2010). Two-stage dynamic signal detection: A theory of choice, decision time, and confidence. *Psychological Review*, *117*(3), 864–901. doi:10.1037/a0019737
9. Van Zandt, T., & Maldonado-Molina, M. M. (2004). Response Reversals in Recognition Memory. *Journal of Experimental Psychology: Learning, Memory, and Cognition*, *30*(6), 1147–1166. doi:10.1037/0278-7393.30.6.1147

10. Busemeyer, J. R., & Bruza, P. (2012). Quantum Models of Cognition and Decision (1st ed.). Cambridge University Press.
11. Diederich, A., & Busemeyer, J. R. (2003). Simple matrix methods for analyzing diffusion models of choice probability, choice response time, and simple response time. Journal of Mathematical Psychology, 47(3), 304-322.
12. Ratcliff, R., & Starns, J. J. (2009). Modeling confidence and response time in recognition memory. Psychological review, 116(1), 59.
13. Ratcliff, R., & Starns, J. J. (2013). Modeling confidence judgments, response times, and multiple choices in decision making: recognition memory and motion discrimination. Psychological review, 120(3), 697.

Figures

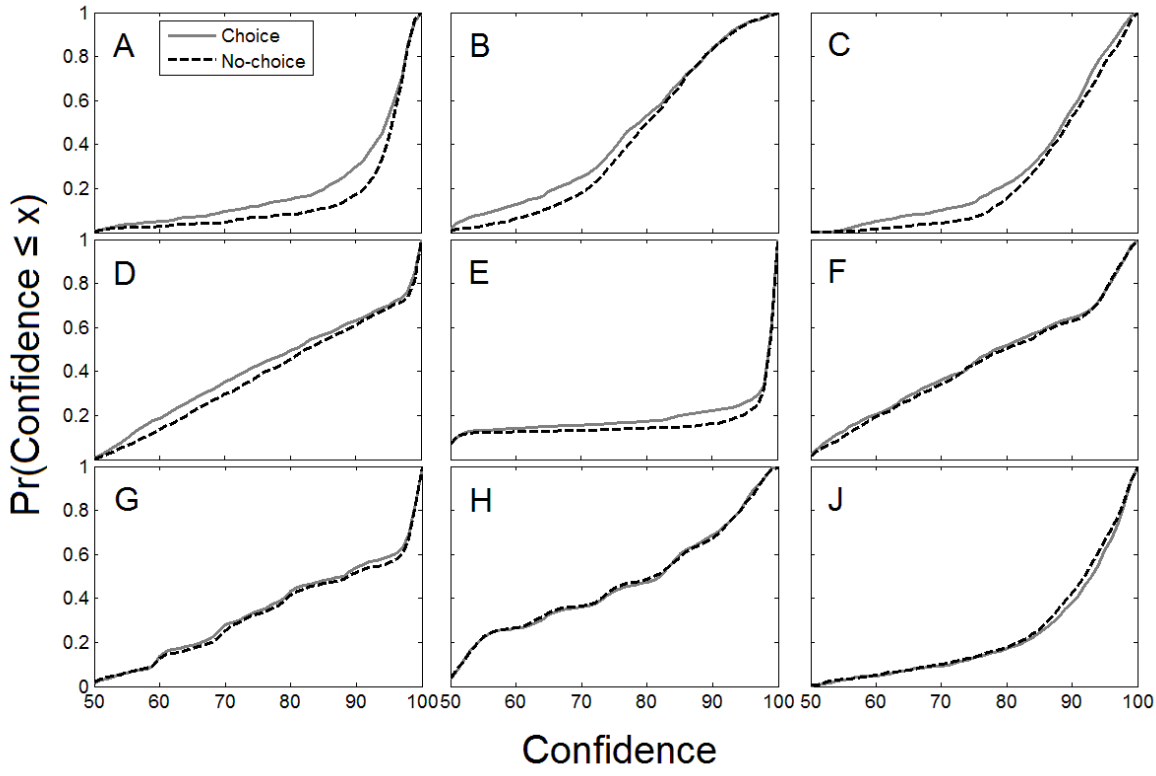

Figure S1: Cumulative distributions of confidence ratings for participants 1-9 (A-J, respectively). Note that participants 1-6 (A-F) showed interference effects, evidenced by the choice condition (gray line) being concentrated closer to 50, resulting in a high cumulative density across the lower confidence levels than the no-choice condition (dotted black line). Participants 7-9 (G-J) did not show significant interference effects, although they trended in the same direction (see Table 1).

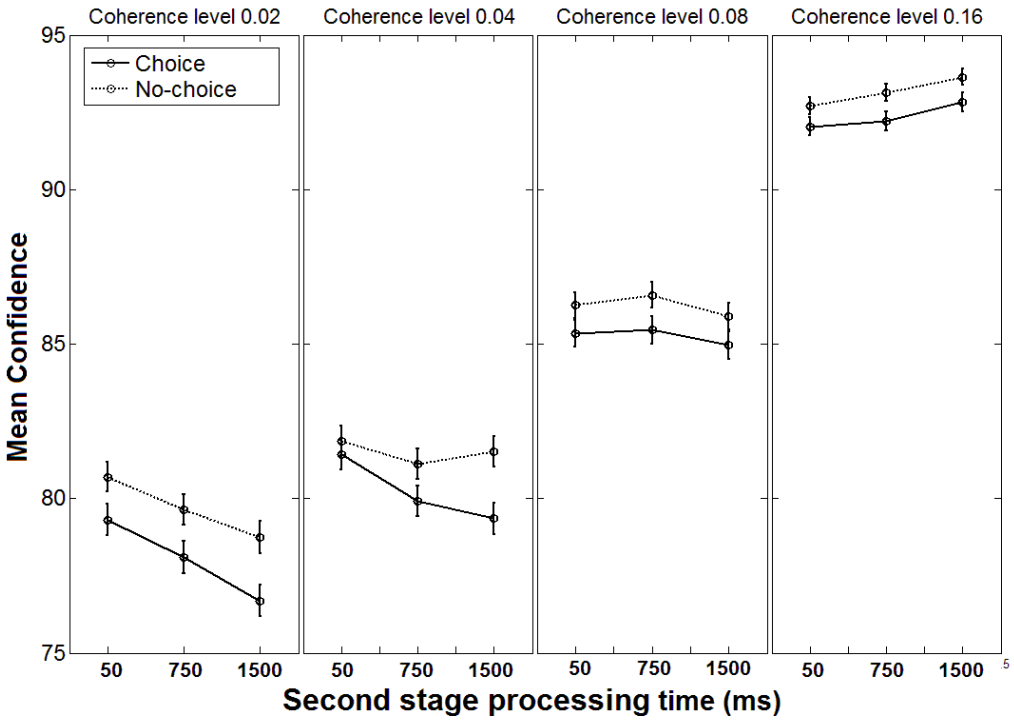

Figure S2: Patterns of mean confidence over time by choice / no-choice, coherence, and IJT. Note the consistently higher confidence in the no-choice condition (interference effect). There is a tendency for confidence to decrease over time at lower coherence levels and increase over time at higher ones, indicating that participants are indeed continuing to process incoming information, though on this scale the highest density interval for the effect includes zero (see Table S1, but also S2 for the estimate on the correctness-based scale)

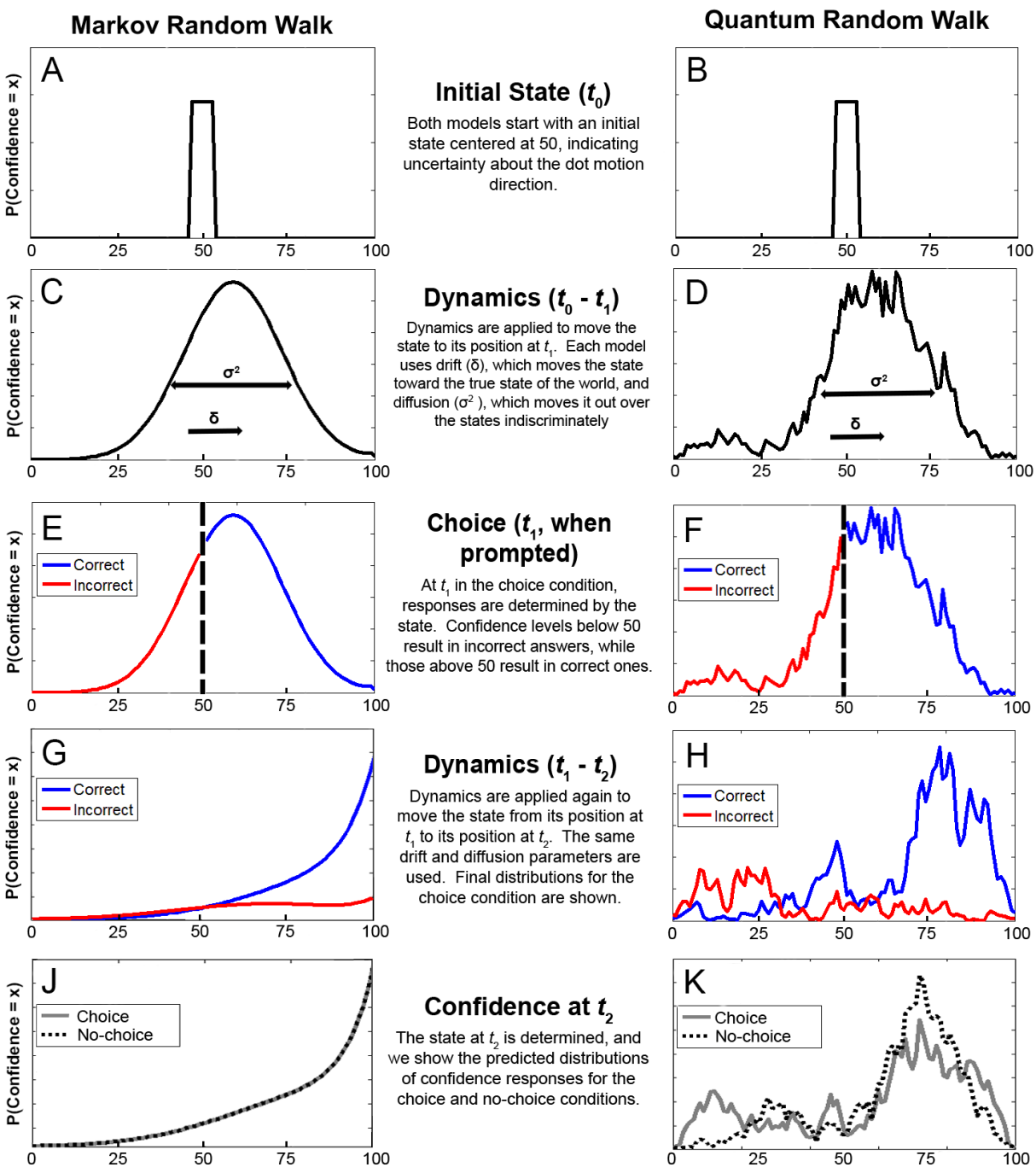

Figure S3: Outline of the dynamics of each model when a rightward moving stimulus is presented. Panels plot hypothetical probability distributions at different time points over different evidence levels, with levels 0–50 corresponding to states that favor the 'left' incorrect response and levels 50–100 corresponding to those that favor the 'right' correct response. Note that in this depiction we assume only 101 rather than 103 states. Each model has an initial state – a mixed state vector in the Markov model, or a superposition state vector in the quantum model – which is centered over 50, indicating uncertainty (A, B). Each one uses a drift **(**δ**)** and diffusion (σ^2)

parameter to describe the average rate of correct evidence and noise accumulated, respectively (C, D), but constructs the operator differently. At t_1, if no choice is cued, then the dynamics continue to be applied. However, if at t_1 a choice is cued, a decision is read out from the MRW, with 'right' being chosen if the evidence is above the decision criterion (E). In the QRW, the probability of choosing 'left' or 'right' is determined by the sum of the squared potentials over those states (F). Moreover, in the QRW, a choice requires that the state be projected onto the corresponding bases (e.g., 50–100 if 'right' is correctly chosen), eliminating the potentials over the states less than 50 and producing a change in the cognitive state. This projection, along with the dynamics applied from t_1 to t_2 (G, H), results in a different distribution of confidence for the choice and no-choice conditions in the QRW (K). However, because no change is made to the state at t_1 due to choice in the MRW, this model predicts that the distributions will be the same for choice and no-choice conditions (J). We present the formal mathematical construction of each model in the main text of the paper, and proofs are supplied in Appendix C.

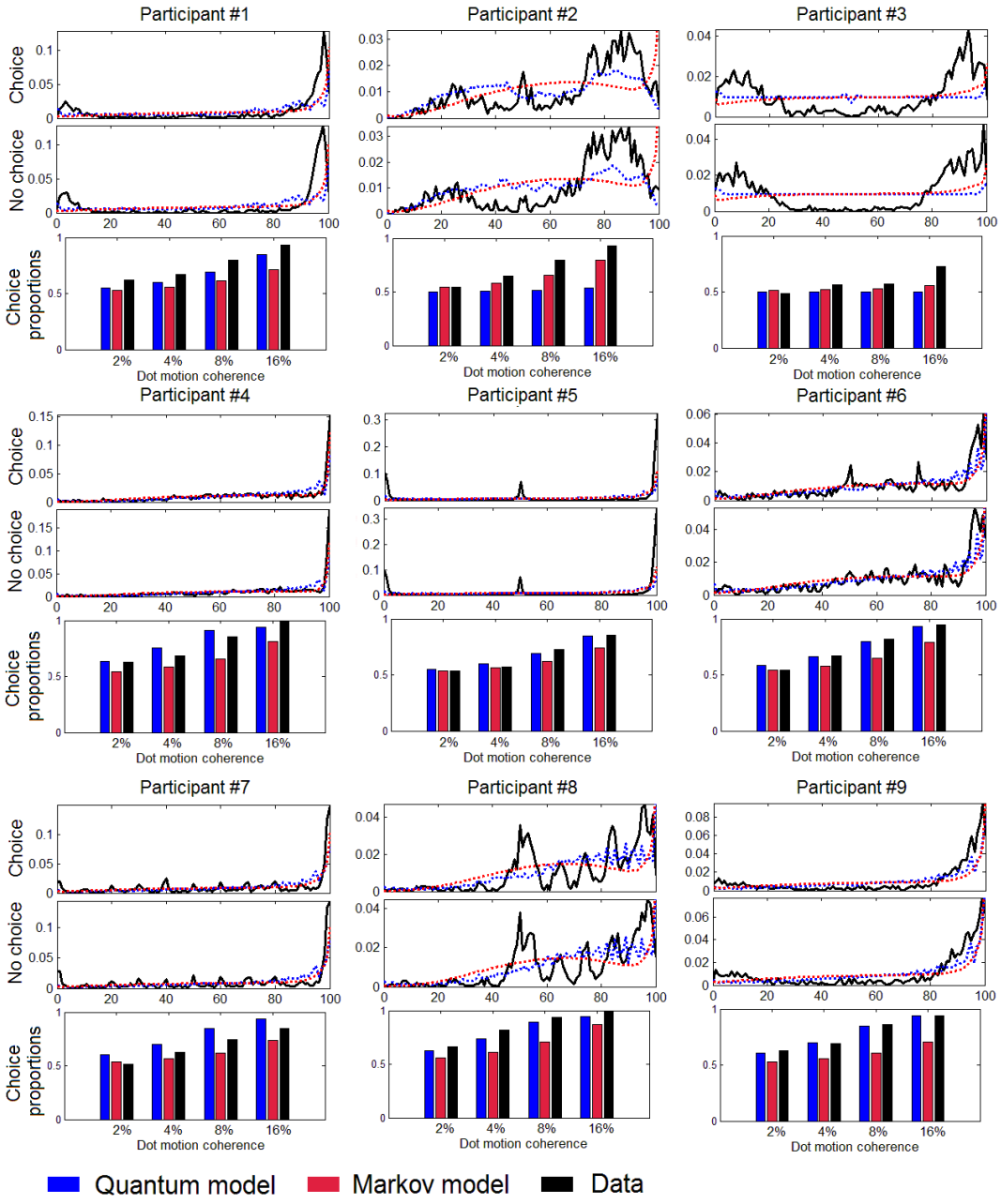

Figure S4: Data along with maximum-likelihood predictions from the Markov and quantum random walk models. Shown are the marginal probability density of confidence responses choice condition and the no-choice condition (top 2 panels for each participant) collapsed across second-stage processing and dot motion coherence manipulations. Also shown are the observed and maximum likelihood predictions for choice proportions in each dot motion coherence condition (bottom panel of each participant). Note that some participants tended to group their responses (e.g. participant #7 used 0/10/20/etc.) – further work incorporating individual differences in response mapping would certainly improve fits for both models, but response mapping does not directly affect interference (see proof in Appendix C).

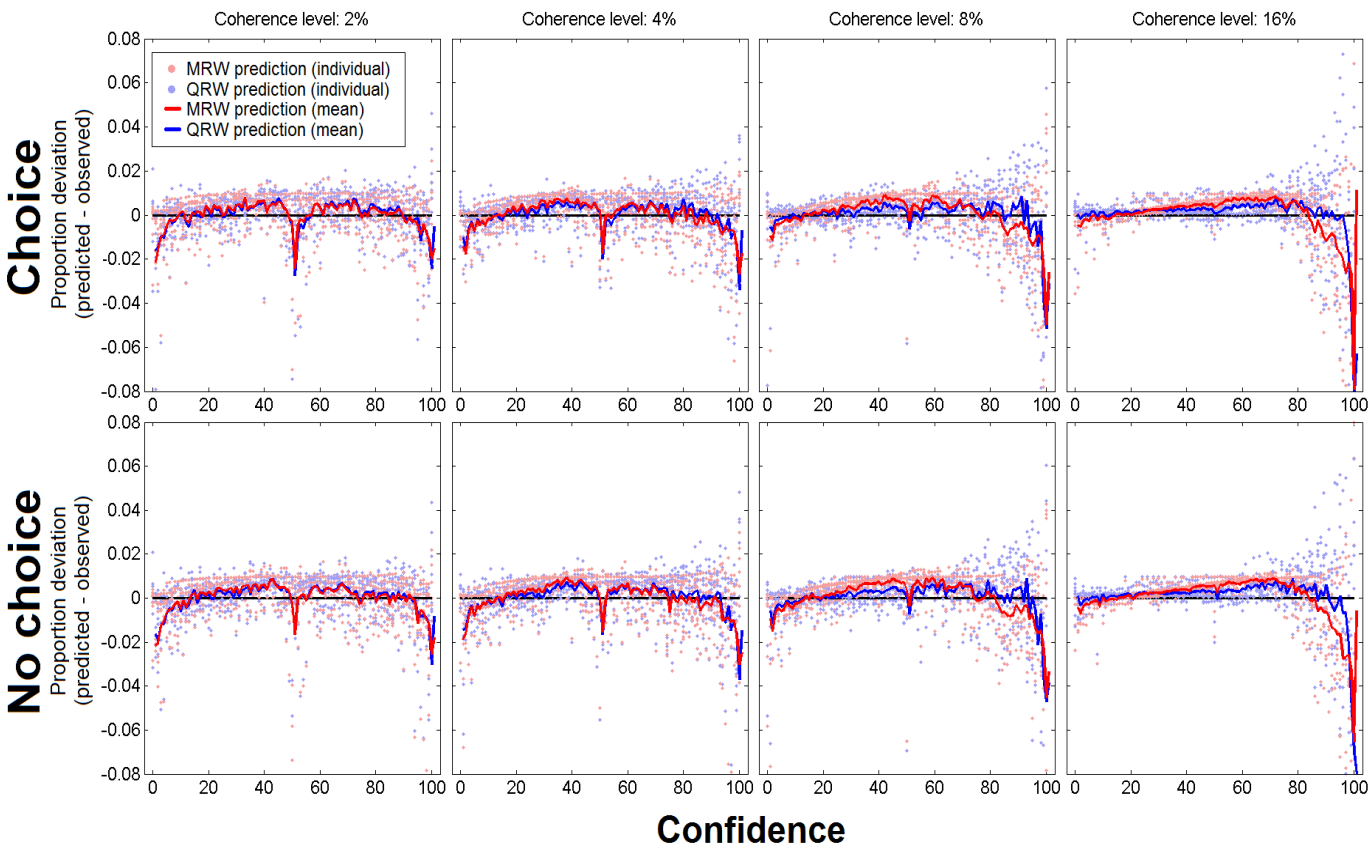

Figure S5: Predicted minus observed proportions of confidence responses from MRW (red) and QRW (blue) models. Within each plot, the zero line corresponds to a perfect fit – i.e., the model did not over- or under-estimate the actual proportion of confidence responses at that level. Values above this line indicate that a model over-estimated the proportion of responses at that confidence level, and values below it indicate underestimation. A dot represents the prediction derived from the maximum likelihood parameters of a model for one participant and coherence level, averaged across second stage processing time. The trend lines plot the mean pattern across all 9 participants, again averaged across second stage processing times. Note that the QRW and MRW both perform reasonably well – with the majority of predictions deviating from observed proportions by less than 0.02 – and offer similar performance at low coherence levels. However, the QRW offers overall closer fits to the data, particularly at high coherence levels, which along with choice proportion fits leads to the superior Bayes factor (note that we do not show the MRW-E, which is again essentially identical to the MRW shown here).

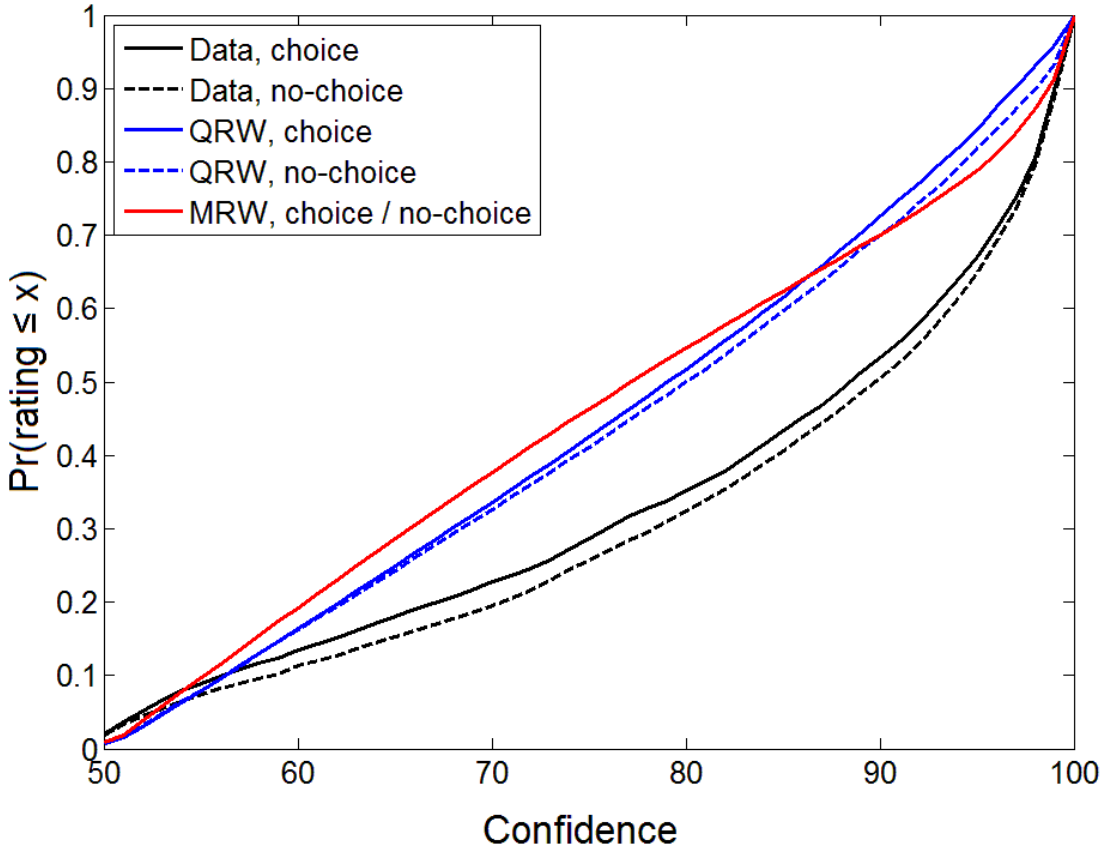

Figure S6: Cumulative distributions of confidence responses in the data (black) and maximum likelihood predictions from the QRW (blue) and MRW (red) for choice and no-choice conditions, averaged across participants, coherence levels, and second stage processing times. There are four things to note: 1) the difference between choice and no-choice conditions in the data (interference effect); 2) a similar effect in the QRW, showing its ability to predict interference; 3) the lack of difference between choice and no-choice in the MRW (no interference); and 4) the closer fit of the QRW to the data relative to the MRW.

However, it is critical to note that the cumulative distribution provides a misleading depiction of the fit of the models, as the deviation between curves shows the accumulated error across many confidence levels. The errors at individual confidence levels are comparatively quite small – a much more accurate impression of fit can be gathered from the probability mass distributions shown in Figures 3 and S4 as well as the deviations in probability mass shown in Figure S5.

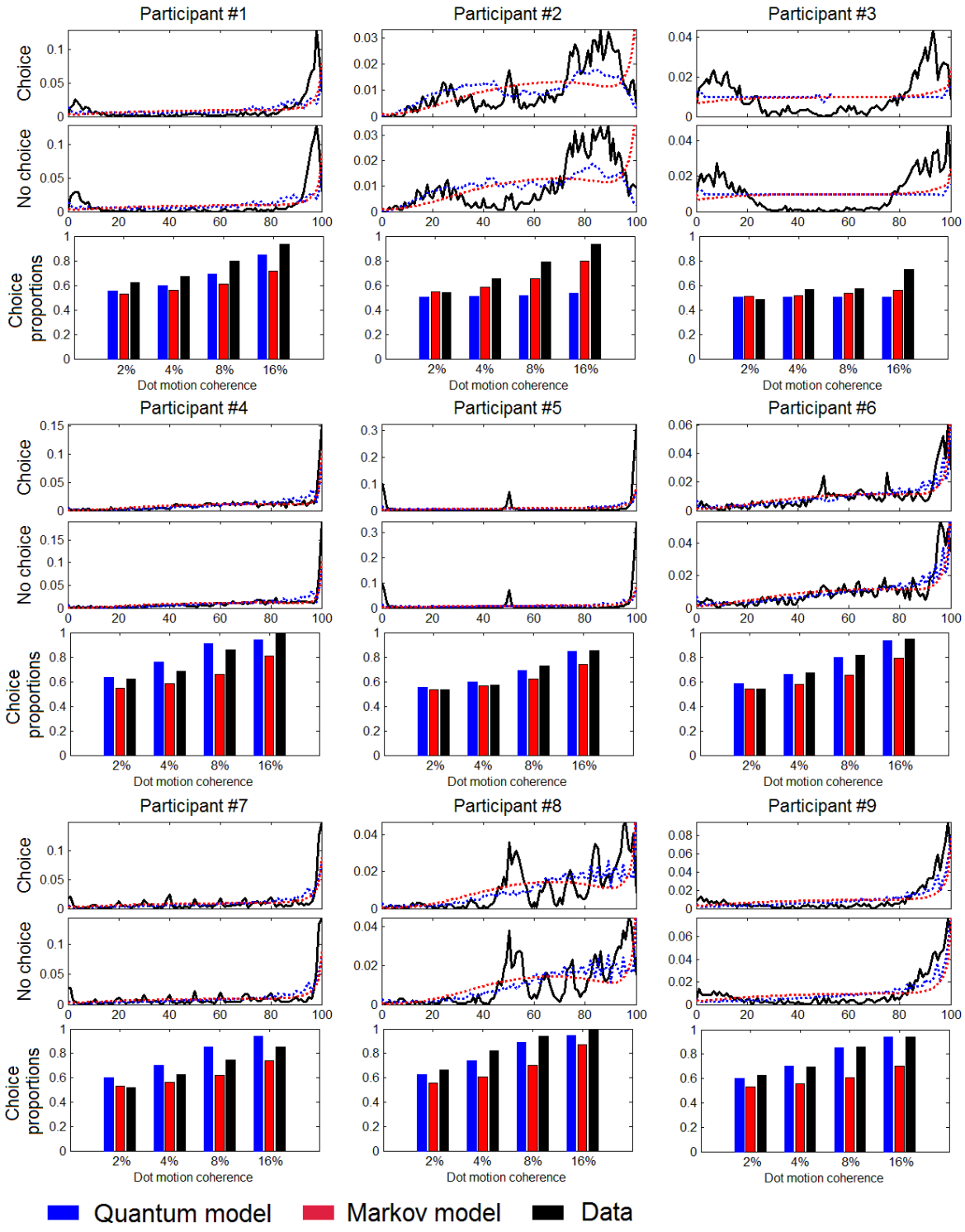

Figure S7: Data and model fits for the QRW and the MRW-E model described in Appendix F. Note that there are nearly no differences when compared to the MRW fits shown in Figure S4 – the only changes are subtle rightward confidence shifts in the no-choice conditions for participants 2, 3, and 6.

Tables

Factor	Mean	95% HDI
Second-stage processing time (SPT)	-0.05	[-0.10 0.00]
Coherence	0.50	[0.04 1.16]
Choice / No-choice (C/N)	-0.11	[-0.18 -0.04]
SPT × C/N	-0.02	[-0.08 0.04]
Coherence × SPT	0.05	[-0.01 0.12]
Coherence × C/N	0.04	[-0.04 0.12]
Coherence × SPT × C/N	0.00	[-0.08 0.08]

Table S1: Main effects and interactions of dot coherence, second-stage processing time (SPT), and the choice / no-choice manipulation (C/N) predicting confidence on the half scale (50-100). Note that the interaction between coherence and SPT is not significant on the half scale, as more evidence for the true state of the world (higher coherence) will increase confidence over time for correct estimates but decrease confidence over time for incorrect ones, and these conflicting patterns wash or cancel each other out

Factor	Mean	95% HDI
Second-stage processing time (SPT)	0.04	[-0.02 0.10]
Coherence	1.15	[0.81 1.49]
Coherence × SPT	0.06	[0.01 0.12]

Table S2: Main effects and interaction of coherence and second-stage processing time (SPT) on confidence, with confidence on a 0 (certain of incorrect direction) to 100 (certain of true direction) scale and transformed into log odds. The values of the interaction of coherence and SPT for each individual, which we use as a measure of post-decisional processing, are presented in Table 1.

	Description	Markov Random Walk Range	Quantum Random Walk Range
Coherence multiplier (μ)	Drift rate is a scalar function of this parameter. The drift rate controls direction and rate of change in evidence stages	[0.1, 3.0]	[1.00, 40.00]
Diffusion (σ^2)	Controls the spread of the accumulating evidence.	[50.00, 250.00]	[1.00, 100.00]
Attenuation (γ)	Sets the relative rate of information processing during the second stage of evidence accumulation	[0.1, 1]	[0.1, 1]
Initial distribution width (w)	Width of initial state.	[1, 51]	[1, 51]

Table S3: The parameters of the Markov random walk and the quantum random walk model and the range of possible values used to calculate the Bayes factor. Note that the coherence multiplier must be multiplied by the percentage of coherently moving dots (2, 4, 8, or 16) and – in the QRW – divided by the number of states we used (103) to get the normalized drift rate.

	Model	
Participant	**QRW**	**MRW**
1	-14521	-14734
2	-11692	-11725
3	-14932	-14801
4	-11586	-11777
5	-10908	-11747
6	-12358	-12581
7	-12031	-11882
8	-12034	-12373
9	-14424	-14574

Table S4: Maximum log likelihood for each model and participant resulting from the grid search used to compute the Bayes factor. Note that the Bayes factor reflects closely the difference between log likelihoods – maximum likelihood estimates tended to be much better than next-best estimates simply due to the large number of data points, giving the priors little influence over the posterior odds.

Participant	Model	Coherence Multiplier (μ)	Diffusion (σ^2)	Width (w)	Attenuation (γ)
1	MRW	2.71	220	51	1
	QRW	24.4	55.45	1	0.235
2	MRW	2.57	230	34	0.415
	QRW	1.00	95.05	48	0.865
3	MRW	0.68	230	51	1
	QRW	1.00	1	51	1
4	MRW	3.00	130	39	0.685
	QRW	23.46	60.4	3	0.1
5	MRW	2.71	240	51	1
	QRW	24.45	55.45	1	0.19
6	MRW	2.86	250	39	0.595
	QRW	22.50	55.45	2	0.235
7	MRW	3.00	250	51	0.865
	QRW	28.30	60.4	2	0.1
8	MRW	2.86	230	28	0.505
	QRW	18.55	65.35	4	0.235
9	MRW	2.57	220	51	1
	QRW	28.30	60.4	2	0.1

Table S5: Maximum likelihood parameter estimates for each participant and model, obtained from the grid search. Note that in most cases, the maximum likelihood estimates were far superior to most other estimates, so we do not include posterior probability density intervals. Also, recall that the coherence multiplier must be multiplied by the percentage of coherently moving dots (2, 4, 8, or 16) and number of states in the QRW (103) to get the drift rate.

Participant	Log Bayes Factor [MRW-E : MRW]	Log Bayes Factor [MRW-E : QRW]
1	-2	-214
2	8	-33
3	-0	131
4	-2	-192
5	-2	-839
6	9	-214
7	-2	146
8	-2	-341
9	-2	-152
Group	4	-1708

Table S6: Model comparison between MRW-E, which includes a parameter for additional processing in the no-choice condition leading to an interference effect, and the MRW as well as the QRW. Positive factors indicate support for the MRW-E.